

Identification of Two Isomers from an Organic Mixture by Double-Stimulated-Echo NMR and Construction of the DOSY Spectra by the Regularized Resolvent Transform Method**

Pierre Thureau,^[a] André Thévand,^[a] Bernard Ancian,^{*,[a]} Philippe Escavabaja,^[b] Geoffrey S. Armstrong,^[c] and Vladimir A. Mandelshtam^[d]

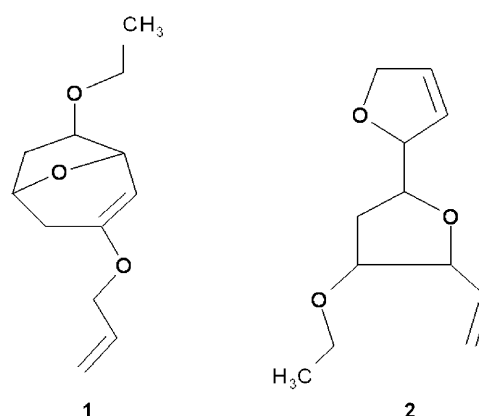
DOSY-NMR experiments were used to characterize two structural isomers that have different shapes, but identical mass fragmentation patterns, from an organic mixture. It is shown that the spherical molecule diffuses faster than the ellipsoidal one. This distinct behaviour is tentatively explained in terms of microfriction effects from the solvent. Finally, to increase the resolution

and efficiency of the 2D DOSY map construction, the data were treated with the regularized resolvent transform method. This method provides good separation for mildly overlapped peaks and requires fewer points than other classical DOSY processing methods.

1. Introduction

The structural characterization of isomers is a challenging task, which is generally achieved through chromatography and mass spectrometry, thus correlating molecular structure and mass spectra.^[1] Sometimes identification is not straightforward by this means, so one has to find an alternative way to differentiate these molecules. Diffusion-ordered spectroscopy (DOSY), as proposed by Johnson^[2] and based on the method of Stejskal and Tanner,^[3] may be used to accomplish this goal. The diffusion coefficient is obtained from the attenuation of the spin echo under the influence of a pulsed magnetic field gradient.^[4] This NMR method has provided interesting results such as separation of multi-component solutions,^[5] characterization of aggregates,^[6] drug design,^[7] chromatographic separation by NMR spectroscopy^[8] and study of molecular interactions, such as hydrogen bond strength.^[9] In a recent application of the method, Lüdemann et al.^[10] were able to show that in neat liquid *N*-methylformamide, the first molecular neighbours to the *cis* conformer are arranged differently to those for the *trans* conformer, thus explaining a retardation of diffusion for the *cis* conformer.

Here, we show by DOSY-NMR spectroscopy the identification of two isomers of general formula $C_{12}H_{18}O_3$ which differ in their shape. These isomers are components of an organic mixture obtained in the course of an organic synthesis: isomer **1**, that is, 3-(allyloxy)-6-ethoxy-8-oxabicyclo[3.2.1]oct-5-ene, is the starting material, and the product, isomer **2**, is an adjacent bis-THF acetogenin (Scheme 1). Unfortunately, mass spectrometry was not able to characterize the two structural isomers as the MS/MS analysis of both compounds revealed the same mass fragmentation pattern. Nevertheless, the two compounds have distinct proton NMR spectra in which high-field resonances strongly overlap, but low-field signals are well separated; the proton spectrum of the starting material **1** is clearly identified.



Scheme 1. Structural formulae of the two isomers.

[a] P. Thureau, Prof. Dr. A. Thévand, Prof. Dr. B. Ancian
Jeune Equipe 2421-TRACES, Université de Provence
Case 512, Centre St Jérôme
13397 Marseille Cedex 20 (France)
Fax: (+33) 491-282-897
E-mail: bernard.ancian@univ-u-3 mrs.fr

[b] P. Escavabaja
UMR CNRS 6178-SYMBIO, Equipe ReSo, Université Paul
Cézanne, Université Aix-Marseille 3
13397 Marseille, (France)

[c] Dr. G. S. Armstrong
Department of Cell and Developmental Biology
University of Colorado Health Sciences Center
Aurora, CO 80045 (USA)

[d] Prof. Dr. V. A. Mandelshtam
Chemistry Department, University of California
Irvine, CA 92697-2025 (USA)

[**] DOSY = diffusion-ordered spectroscopy.

In addition, by use of the sAM1 modelling method for optimizing the geometries of the two isomers, it is shown that they differ only slightly in their shapes (Figure 1): **1** is a globular spheroidal molecule with an average radius of 450 pm (extreme lengths are 1010, 840 and 830 pm), whereas **2** is a rather prolate ellipsoid with a long semi-axis of 605 pm and a short semi-axis of 380 pm (extreme lengths are 1210, 750 and 760 pm). These values correspond to molecular volumes of about $374 \times 10^6 \text{ pm}^3$ ($\pm 8 \times 10^6 \text{ pm}^3$) in both cases. According to the general Stokes–Einstein equation,^[11] the difference in shape of the two isomers should lead to different translational diffusion coefficients D .

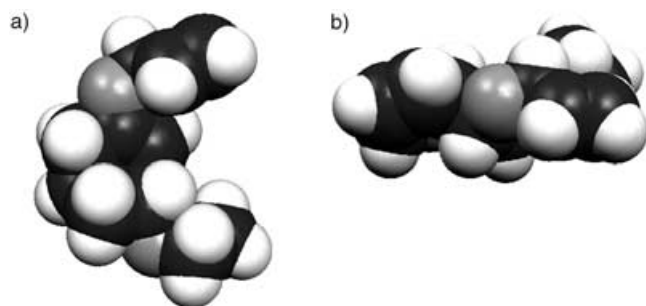


Figure 1. The sAM1 optimized structure of the two isomers: a) the spheroidal isomer **1** and b) the prolate isomer **2**. The carbon atoms are coloured in black, hydrogen in white and the oxygen atoms in grey.

Herein, we discuss the applicability of the DOSY experiment for determining the diffusion coefficients of isomers in a liquid mixture. The reconstruction of the 2D DOSY spectrum is performed using the regularized resolvent transform (iRRT)^[12] (the “i” in its acronym indicates the application along the imaginary frequency axis). Although it is computationally very inexpensive, the iRRT method appears very efficient in terms of both resolution and sensitivity for spectra with pure multi-exponential decays in the diffusion dimension.

2. Results and Discussion

2.1. Diffusion Coefficients of the Isomers

The two diffusion coefficients were calculated using the peaks at 4.55 ppm for **2** and at 5.25 ppm for **1**. These two peaks are well separated from other resonances, so they are described by a mono-exponential function. Data were analysed by plotting the signal intensities (areas) as a function of the gradient strength, followed by non-linear least-squares fitting of the resulting decay curves. For internal consistency, we checked the method by calculating the diffusion for CDCl_3 , which was used as a solvent, from the peak at 7.24 ppm: the value $D(\text{CDCl}_3) = 2.36 \times 10^{-9} \text{ m}^2 \text{ s}^{-1}$ obtained is in agreement with that of $2.27 \times 10^{-9} \text{ m}^2 \text{ s}^{-1}$ reported in international tables.^[13] The diffusion coefficient for **2** was measured as $D(2) = 1.18 \times 10^{-9} \text{ m}^2 \text{ s}^{-1}$ and for **1** as $D(1) = 1.38 \times 10^{-9} \text{ m}^2 \text{ s}^{-1}$ (Figure 2), with experimental accuracy better than $\pm 5\%$.

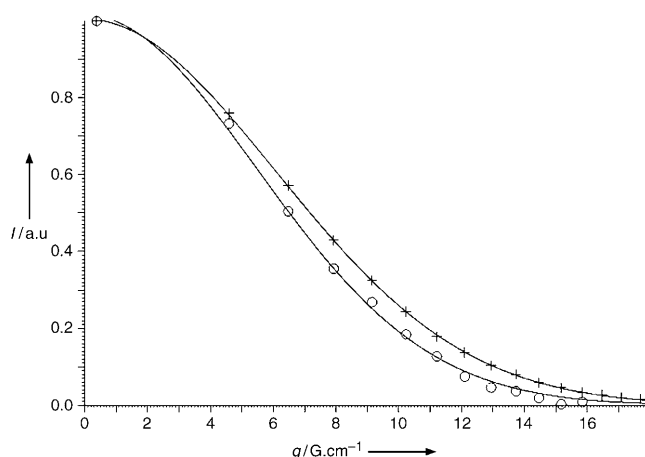


Figure 2. Plot of the signal intensity I as a function of the gradient strength g . Diffusion measurements are obtained on the Gaussian decay fitted by a non-linear least-squares algorithm. The circles represent the normalized signal integral of the peak at 5.25 ppm (isomer **1**) and the crosses, the peak at 4.55 ppm (isomer **2**).

The translational diffusion coefficient D of a solute in an infinitely dilute solution is traditionally estimated by the Stokes–Einstein^[11] Equation (1):

$$D = \frac{k_B T}{6\pi\eta r} \quad (1)$$

where k_B is the Boltzmann constant, T is the absolute temperature, η is the shear viscosity of the solvent and r is the radius of the solute particle. However, the failure of Equation (1) is well documented:^[14] the original theory associated with the Stokes–Einstein equation is only valid when the size of the solute molecules is large relative to that of the solvent molecules, so that the solvent can be treated as a hydrodynamic continuum. Significant effort has been devoted to adapting and extending this theory to the cases where the sizes of the solute and solvent molecules are on the same order of magnitude. Gierer and Wirtz's^[15] microfriction theory represents the only theoretical modification where strong stick hydrodynamic boundary conditions are relaxed. For the latter case, by assuming spherical shapes for both the solute and the solvent molecules, Equation (1) still holds provided the right-hand side is multiplied by a microfriction factor f_t as defined by Equation (2):

$$f_t = \frac{3r_2}{2r_1} + \frac{1}{1 + (r_2/r_1)} \quad (2)$$

where r_1 and r_2 are the solute and solvent radii, respectively. Note that, in this case, the microfriction factor only depends on the ratio r_1/r_2 .

For the nearly spherical solvent CDCl_3 , a Van der Waals volume of about $71 \times 10^6 \text{ pm}^3$ is calculated from the atomic increments reported by Edward,^[16] which therefore gives $r_2 \approx 256 \text{ pm}$. Introducing this value into Equation (2), together with $r_1 = 450 \text{ pm}$ for isomer **1**, we obtain a microfriction factor $f_t = 1.49$. Given a viscosity of 0.510 cP for CDCl_3 at 300 K,^[13] and

using Equation (1) corrected by the factor f_v , we obtain a diffusion coefficient $D(1) = 1.44 \times 10^{-9} \text{ m}^2 \text{ s}^{-1}$ which compares well with the experimental value of $1.38 \times 10^{-9} \text{ m}^2 \text{ s}^{-1}$.

For the prolate isomer **2**, the theory becomes more cumbersome because the anisotropy in the molecular diffusion prevents the use of a simple microfriction factor. Nevertheless, a very simple but approximate expression, as given by Perrin,^[17] shows that the diffusion coefficient of the ellipsoid is dependent on the ratio ρ of its axes under stick boundary conditions. With $\rho = 380/605 = 0.63$, Equation (102) of Perrin^[17] thus gives $D_p/D_s = 0.98$ for the ratio of the diffusion coefficient (D_p) of isomer **2** to that (D_s) of isomer **1**, which is clearly greater than the experimental value of $D(2)/D(1) = 0.86$. It is evident that such a discrepancy results from approximations in Perrin's equations where rotation–translation coupling is neglected.^[17] Putting the long semi-axis of the prolate isomer **2** for the radius r_1 in Equation (2) yields the microfriction factor $f_t = 1.34$ and diffusion coefficient $D_p = 0.96 \times 10^{-9} \text{ m}^2 \text{ s}^{-1}$. As expected, this calculated value is now lower than the experimental value $D(2) = 1.18 \times 10^{-9} \text{ m}^2 \text{ s}^{-1}$. To try and improve this result, we considered the free rotation around the C–O–CH₂–CH₃ moiety of the molecule and calculated an average shape of this isomer. Weighting with the correct energy calculated for each conformer, the average geometry of **2** gives a long semi-axis of 585 pm and a microfriction factor of 1.35, which results in a diffusion coefficient of $1.01 \times 10^{-9} \text{ m}^2 \text{ s}^{-1}$.

Such an analysis seems to indicate that there is a strong rotation–translation coupling in the translational diffusion mode of the prolate isomer **2**.

2.2. Construction of the DOSY Map by the iRRT Method

To immediately visualize the effects under study we constructed a DOSY-NMR map. DOSY processing provides a 2D spectrum with NMR chemical shifts in one dimension and diffusion coefficients in the other. In DOSY-NMR experiments, the required spectral information cannot be obtained by conventional means (such as Fourier transformation) as the spectral separation in the diffusion dimension requires one to implement either a multi-exponential fit or an inverse Laplace transform, both of which are ill-posed problems.

In the most widely used scheme the multi-dimensional DOSY data are Fourier transformed in all but the diffusion dimension, followed by a single-exponential fit in the diffusion dimension. While effective for well-dispersed spectra, this scheme is known to be unstable for overlapping regions. Several methods have been developed to deal with this shortcoming.^[18] We chose to construct the DOSY map using the iRRT^[12] method, which has proved to be effective for treating moderately overlapping data.

The regularized resolvent transform (RRT)^[19] is a processing scheme developed for multi-dimensional NMR experiments. It is based on the assumption that the two-dimensional time domain data, $C(n, m)$, can be represented in the form [Eq. (3)]:

$$C(n, m) = \Phi^T U^n A^m \Phi \quad (3)$$

with two commuting time-evolution operators U and A . Here, Φ represents the fictitious initial state of the system. In the case of the filter diagonalization method (FDM),^[20] U and A are diagonalized to extract the spectral parameters. However, by using the analytical form of the discrete Fourier transform (and correspondingly the inverse Laplace transform) of $C(n, m)$ and employing the assumption of Equation (3), a spectral representation can be obtained. In the case of DOSY, only the real data in the diffusion dimension are available, so the pseudo-absorption spectral representation is used to obtain approximate double-absorption lineshapes [Eq. (4)]:

$$A(\omega, D) = \left| \Phi^T \frac{1}{(1-U/u)^2} \frac{1}{(1-A/\lambda)^2} \Phi \right| \quad (4)$$

where $u = e^{-i\tau\omega}$ and $\lambda = e^{\beta^2 \Delta D}$; τ and D are the dwell times, and β accounts for the Gaussian behaviour of the diffusion. Matrix representations of the operators can be constructed from the data, and reduced to linear least-squares problems to produce a multi-dimensional spectral estimate according to Equation (5):

$$A(\omega, D) = |C^T R_1^{-1}(\omega) U_0 R_1^{-1}(\omega) U_0 R_2^{-1}(D) U_0 R_2^{-1}(D) C| \quad (5)$$

where C , U_0 , $R_1(\omega)$ and $R_2(D)$ are the matrix representations of the elements of Equation (4) (data matrices). While solutions of these least-squares problems are unstable, several robust regularization techniques for these problems exist, which makes the RRT an ideal method to treat very ill-conditioned problems. In DOSY spectroscopy, the proton time dimension is composed of complex frequencies, and the diffusion dimension contains real time decays. The RRT is a multi-dimensional process by nature, so it can be easily adapted to treat this form of data, to give the so-called iRRT method.^[12]

We emphasize here that some important advantages of this method for acquisition and processing in the DOSY experiments include the following: it does not require a large number of points in the diffusion dimension to achieve a high-resolution spectral estimate, which allows one to substantially reduce the experimental times; it also allows the separation of overlapping components without having to guess the number of compounds present in the mixture (i.e. the latter is not an input parameter of the iRRT). Due to the nature of the regularization and the ability to process all dimensions of the signal at once, the iRRT is often able to achieve resolution in cases where other methods have difficulties.

Figure 3 shows a comparison of the 2D DOSY maps constructed using a non-linear least-squares fitting to a mono-exponential decay and by the iRRT method. With the iRRT method the peaks are relatively sharp even in the region of significant overlap from the two compounds. Moreover, the iRRT is able to clearly separate the solvent from the two isomers. As a result, two well-separated lines across the centres of the computed peaks along the chemical shift dimension can be drawn for each isomer.

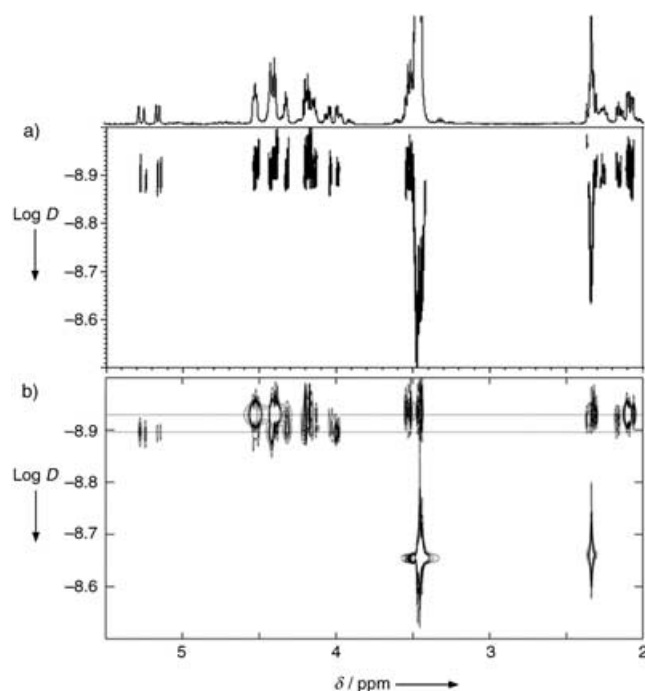


Figure 3. Comparison of the DOSY spectra obtained by a mono-exponential fit (a) and by the iRRT method (b) with the same contour levels. In contrast to the standard DOSY method, one can distinguish the two isomers with the iRRT method. In addition, a separation between the residual solvents and the products is also clearly seen. Peaks at 2.35 and 3.48 ppm are artefacts from the toluene (CH_3 peak) and the diethyl ether (CH_2 peak), respectively, which have nearly identical diffusions in CDCl_3 .

3. Conclusions

We were able to characterize two structural isomers using a simple diffusion NMR experiment, processed by the robust iRRT method. It is shown that the spheroidal isomer diffuses faster than the ellipsoidal isomer. Moreover, the value measured for its experimental diffusion coefficient is qualitatively well interpreted by the simple microfriction theory of Gierer and Wirtz. Nevertheless, this crude theory fails to approximate the slow diffusion of the ellipsoidal isomer because of a strong translation–rotation coupling in its displacement.

Experimental Section

All spectra were acquired at 300 K on a Bruker Avance spectrometer operating at the proton frequency of 500.13 MHz and equipped with an inverse ^1H cryoprobeTM. A z gradient, shaped to a half-sine bell, was used with a maximum intensity of $55 \times 10^{-2} \text{ T m}^{-1}$. The sample was dissolved in neat CDCl_3 (99.96% deuterated). The DOSY experiments were performed using the double-stimulated echo (DSTE) sequence, which is known to refocus the effects of constant flow velocity.^[21] The diffusion delay time (Δ) was 200 ms and the gradient pulse length (δ) was 2 ms. The data for measuring the diffusion coefficient were acquired with 32768 points in the direct dimension, and 16 points in the diffusion dimension. The data for the DOSY spectrum were collected with equal g^2 spacing to enforce the exponential behaviour required by the iRRT;

32768 points were collected in the direct dimension, and only 8 points were collected in the diffusion dimension. The diffusion coefficients were calculated by the Simplex algorithm from the Bruker software Xwinmr 3.5. For comparison purposes, the DOSY data were also processed by applying the Fourier transform to the acquisition dimension followed by performing an exponential fit for each frequency point. The algorithm from the Bruker software Xwinmr 3.5 was used, and the decay curves were fitted to a mono-exponential decay with the Levenberg–Marquardt non-linear least-squares algorithm.

The error in the fitting was $\pm 2\%$, whereas a statistical error of $\pm 5\%$ was obtained from several measurements. Notably, in contrast to single- and multi-exponential-type methods, the peak width in the diffusion dimension for the iRRT was related to the degree of regularization of the data rather than the error of the fit.

Acknowledgements

We thank Dr V. Ledentu for his help in the molecular modelling. We are much indebted to Professor P. Stilbs for drawing our attention to reference [10]. V.A.M. acknowledges the NSF support, grant CHE-0414110. He is an Alfred P. Sloan research fellow.

Keywords: diffusion • diffusion-ordered spectroscopy • isomers • NMR spectroscopy • signal analysis

- [1] J. H. Beynon, *Mass Spectrometry and its Applications to Organic Chemistry*, Elsevier, Amsterdam, **1960**.
- [2] C. S. Johnson, Jr., *Prog. Nucl. Magn. Reson. Spectrosc.* **1999**, *34*, 203–256.
- [3] E. O. Stejskal, J. E. Tanner, *J. Chem. Phys.* **1965**, *42*, 288–292.
- [4] P. Stilbs, *Prog. Nucl. Magn. Reson. Spectrosc.* **1987**, *19*, 1–45.
- [5] K. F. Morris, C. S. Johnson, Jr., *J. Am. Chem. Soc.* **1992**, *114*, 3139–3141.
- [6] K. F. Morris, C. S. Johnson, Jr., *J. Am. Chem. Soc.* **1993**, *115*, 4291–4299.
- [7] M. Lin, M. J. Shapiro, J. R. Wareing, *J. Am. Chem. Soc.* **1997**, *119*, 5249–5250.
- [8] S. Viel, F. Ziarelli, S. Caldarelli, *Proc. Natl. Acad. Sci. USA* **2003**, *100*, 9696–9698.
- [9] G. S. Kapur, E. J. Cabrita, S. Berger, *Tetrahedron Lett.* **2000**, *41*, 7181–7183.
- [10] L. Chen, T. Gross, H. D. Lüdemann, H. Krienke, R. Fischer, *Naturwissenschaften* **2000**, *87*, 225–228.
- [11] A. Einstein, *Investigation on the Theory of the Brownian Movement*, Dover, New York, **1956**.
- [12] G. S. Armstrong, N. M. Loening, J. E. Curtis, A. J. Shaka, V. A. Mandelshtam, *J. Magn. Reson.* **2003**, *163*, 139–148.
- [13] Landolt-Börnstein, *Zahlenwerte und Funktionen*, Vol. II, Part 2, Springer, Berlin, **1962**.
- [14] J. V. Tyrrell, K. R. Harris, *Diffusion in Liquids: A Theoretical and Experimental Study*, Butterworths, London, **1984**.
- [15] A. Gierer, K. Wirtz, *Z. Naturforsch. A* **1953**, *8*, 532–538.
- [16] J. T. Edward, *J. Chem. Educ.* **1970**, *47*, 261–270.
- [17] F. Perrin, *J. Phys. Radium* **1936**, *7*, 1–11.
- [18] B. Antalek, *Concepts Magn. Reson.* **2002**, *14*, 225–258.
- [19] J. Chen, A. J. Shaka, V. A. Mandelshtam, *J. Magn. Reson.* **2000**, *147*, 129–137.
- [20] V. A. Mandelshtam, *Prog. Nucl. Magn. Reson. Spectrosc.* **2001**, *38*, 159–196.
- [21] A. Jerschow, N. Müller, *J. Magn. Reson.* **1997**, *125*, 372–375.

Received: April 7, 2005

Published online on July 20, 2005